Mechanical excitation of rodlike particles by a vibrating plate

Torsten Trittel,[1] Kirsten Harth,[1,2] and Ralf Stannarius[1]

[1]*Otto-von-Guericke-University, Institute of Experimental Physics, Universitätsplatz 2, D-39106 Magdeburg, Germany*

[2]*Universiteit Twente, Physics of Fluids and Max Planck Center for Complex Fluid Dynamics, P.O. Box 217, 7500 AE Enschede, The Netherlands*

(Received 6 March 2017; published 21 June 2017)

The experimental realization and investigation of granular gases usually require an initial or permanent excitation of ensembles of particles, either mechanically or electromagnetically. One typical method is the energy supply by a vibrating plate or container wall. We study the efficiency of such an excitation of cylindrical particles by a sinusoidally oscillating wall and characterize the distribution of kinetic energies of excited particles over their degrees of freedom. The influences of excitation frequency and amplitude are analyzed.

DOI: 10.1103/PhysRevE.95.062904

I. INTRODUCTION

A common method to supply kinetic energy to an ensemble of particles to study their statistical dynamics is the mechanical excitation of the individual particles by vibrating container walls [1–3]. Often, submonolayers of grains are shaken on a horizontal plate in two-dimensional (2D) or quasi-2D experiments. In three dimensions, one or more container walls can be vibrated, or the whole container is shaken. In the majority of such experiments, spherical particles have been investigated (see, for example, Refs. [1–19]). Most studies were performed in vertically shaken containers. Thereby, the granulate is fluidized, and a granular temperature can be assigned as a measure of kinetic energy. One finds interesting phenomena like convective flow [13,14], localized structures [15], segregation [16], and others. At sufficiently strong shaking, the grains lose permanent contact with their neighbors, a so-called "granular gas" state is reached. New phenomena like clustering [17], directed particle transport [18], or Leidenfrost-like layering [19] are observed. Under normal gravity, this requires a substantial level of excitation.

An interesting aspect of granular gases is their dynamics at low excitation or without external energy supply, as model systems for stochastic multiparticle dynamics. Such experiments give insight, e.g., into clustering mechanisms that are the basis of fundamental structure formation in the universe (see, e.g., Ref. [20]). Without energy supply, dissipative collisions of grains in a granular gas lead to a permanent loss of kinetic energy, so-called "granular cooling." This process was analyzed theoretically by Haff [21] for a homogeneous granular gas of identical spherical grains with given restitution coefficient.

Some three-dimensional (3D) experiments with granular gases have been performed in microgravity, where relatively low excitation strengths are sufficient to maintain stationary states [5,6,22–29]. In these experiments, observability and interaction efficiency pose conflicting constraints: The particle number density must be high enough to achieve sufficiently frequent collisions among particles before they hit a container wall. Their mean free paths must be small compared to the container size. On the other hand, the observation of the particles requires a sufficiently low particle density so that the *optical* mean free path allows us to observe not only the particles in a thin region in the front. This problem can be resolved partially when cylindrical or other elongated grain shapes are used. With such a particle geometry one can shorten the mean free path between particle collisions (related to the rod length) while keeping the optical path length (which equally involves length and width of the grains) sufficiently long.

In microgravity experiments with rodlike particles, equipartition of the kinetic energy between the translational and rotational degrees of freedom was investigated both experimentally [26–29] and theoretically [30–35]. One of the important open questions of the study of rods is the relation between excitation parameters and energy supply to the system. Since this energy transfer can be traced back to individual collisions of grains with the vibrating container walls, it can be analyzed by measuring impact and rebound characteristics of individual rodlike particles on a vertically vibrated plate. This problem will be addressed here experimentally.

Impact and rebound of spheres on vibrating plates have been studied in numerous publications (e.g., Refs. [36–38]). The standard experiment is the observation of jumping spheres on a horizontal sinusoidally oscillating plate under normal gravity. Such objects can be described in good approximation by one single degree of freedom. Rotations can practically be neglected, and lateral motion can be completely separated from the relevant dynamics in a vertical direction. This allows to reduce the equations of motion to a single one-dimensional differential equation. Nevertheless, the behavior of this nonautonomous system is complex enough. Excitation parameters as well as the restitution coefficient determine different dynamic regimes, from regular periodic jumps to period doubling and chaotic motion. There are only few studies of nonspherical particles in this context. In particular, a few experiments and theoretical work on dumbbell-shaped dimer particles [39,40], trimers [41,42], and springs [43] have been published, mainly directed to the analysis of the dynamic regimes and lateral migration of the objects. A pioneering experimental and theoretical work devoted specifically to cylindrical (more exactly, spherocylindrical) particles bouncing on a vibrating plate was published by Wright *et al.* [44]. This study revealed important differences between the bouncing statistics of spherical particles and cylinders, and it demonstrated the complexity of the dynamics. In particular, the coupling of rotational and translational motions leads to stochastic dynamics for almost all values of the excitation parameters. Quasiperiodic orbits were identified only at very low excitation amplitudes. The kinetic energy distribution was analyzed. Statistics of the times between impacts were evaluated as well as details like flipping processes about the

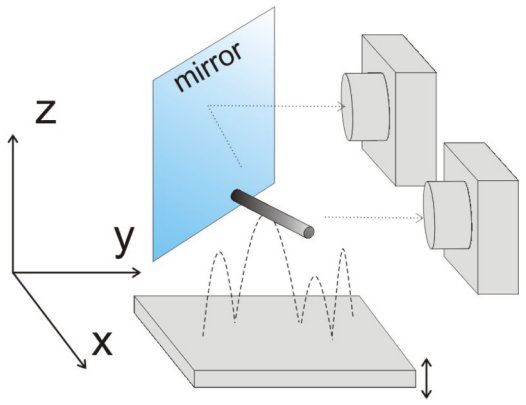

FIG. 1. The figure sketches the setup with the vibrating plate, a mirror, and two cameras with observation axes along x and y, respectively, and it defines the coordinate system used. Two vertical white-coated aluminium side walls and two ITO-coated acrylic glass side walls prevented the particle from leaving the plate. These walls are not shown.

particle short axes. Comparison with numerical simulations demonstrated the successful applicability of MD simulations. Irrespective of a rich collection of quantitative data, this study did not discuss the parameters that are interesting in the context of granular gas driving, i.e., quantitative relations between rotational and translational degrees of freedom and the dependence of the efficiency of excitation on driving parameters.

Wright *et al.* used steel rods with diameters from 1 to 3.2 mm, lengths from 6 to 24 mm and aspect ratios between ≈2 and 20. They observed the particles with one fast camera, which poses some restrictions on the evaluation of trajectories. In particular, rotational motions can be identified only in a 2D projection. The present study extends the observation by a second camera for stereoscopic analysis, so that the full 3D trajectories and rotations become accessible.

II. EXPERIMENT

The setup is sketched in Fig. 1. A white-coated quadratic aluminium ground plate (80 mm × 80 mm, 3 mm thick) was actuated by a voice coil. The cameras (GoPro Hero 3+ Black Edition) were able to record images at frame rates of 240 fps (848 × 480 pixel). The spatial resolution is better than 0.2 mm/pixel. A slight disadvantage of the cameras is that they record images line-by-line, so that very fast rods may appear slightly curved in the images. This artifact is negligible with respect to the uncertainties of the 3D image reconstruction procedure. From the two perspective views, the positions and orientations of particles were reconstructed using a Matlab Camera Calibration Toolbox (Caltech). The vertical oscillations $z_p(t) = A \sin 2\pi f t$ of the bottom plate were driven with frequencies f in the range between 15 and 40 Hz, amplitudes A were chosen between 1 and 5 mm. Characteristic excitation parameters are the maximum plate velocity $v_{\max} = 2\pi f A$ and the maximum plate acceleration $\Gamma_{\max} = (2\pi f)^2 A$. Excitation sequences with desired amplitudes and frequencies were generated with a computer program, and parameters were confirmed by evaluation of the recorded videos.

The particles are insulated wires with outer diameters of 1.3 mm and lengths of 7.5 and 15 mm. Rod ends are cut flat. The choice of material was motivated by its earlier successful usage in microgravity experiments [26–29]. There is no principal difference to any noncomposite (e.g., all-metal) rodlike particles. The advantage of the nonmetallic insulating layer was the uniform reflectivity and absence of metallic optical reflexes, which are problematic for the automatic particle detection. The metal core seems to help prevent electrostatic charging (see below). The longer particles with aspect ratio 11.5 have a mass of 56 mg, and a moment of inertia for rotation about the short axes, $I_\perp = 1.06 \times 10^{-9}$ kg/m^2. The moment of inertia for rotation about the long axis is two orders of magnitude smaller. For the shorter rods with aspect ratio 5.7, $m = 28$ mg and $I_\perp \approx 0.135 \times 10^{-9}$ kg/m^2. A restitution coefficient $\varepsilon \approx 0.54$ of the 15 mm particles has been determined earlier from drop experiments [26].

During the experiments, we did not find noticeable electrostatic effects that influenced the wires. The trajectories were not prone to "aging" caused by static charges on the particles. In similar experiments performed for test purposes with glass rods of similar sizes, electrostatic charging proved to be a considerable problem.

An additional experimental test was performed with copper cylinders (1 mm diameter, 15 mm length, 105 mg mass, $I_\perp = 1.98 \times 10^{-9}$ kg/m^2), where we checked whether the results obtained for the structured wire pieces can be generalized to homogeneous rods.

For each set of parameters, we have recorded 30 000 frames (125 s) of the trajectories. The evaluation of these trajectories revealed that the centers of mass performed exact parabolas within the experimental resolution during the jumps. The rotation proved to be constant between two subsequent collisions with the ground plate, the center-of-mass velocities at impact, v_0, were related precisely to the jump height h_0 by $h_0 = v_0^2/(2g)$. The sum E_z of kinetic energy of vertical motion and potential energy relative to the mean plate height is constant during each jump; it suffices to measure the jump height to determine this quantity. There is no exchange of energies between the three components, horizontal motion (E_{xy}), vertical motion (E_z), and rotational motion ($E_{\rm rot}$), during individual jumps. We further note that we did not try to resolve rotations of the rods about their long axis. This degree of freedom is not excited directly by the vibrating plate technique. We assume that it is equally inactive as the translational horizontal motions, which are not excited directly either. Another consequence of the rotational symmetry of the rods is that we cannot distinguish between the two degrees of freedom of rotations about the two short axes; we observe only their sum.

III. RESULTS

A. Energy distribution

We are not interested here in the analysis of regularity of the particle motion, which has been described by Wright *et al.* [44]. Periodic motions, as they are often found for spherical grains, are practically absent in the rod experiments. Moreover, they would play no role in zero gravity investigations, since the particle leaves the plate without return unless it collides

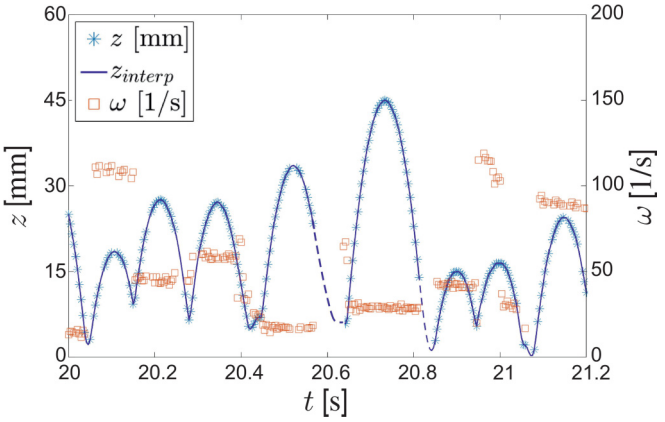

FIG. 2. Exemplary positions and rotational velocities of a 15 mm jumping rod at 30 Hz excitation. The sign of the rotations is not considered in this plot. Rotation rates are constant within each jump, except in the seventh full jump in this image, where the particle collided with the side wall, causing a drop of the rotation rate. In case of such very rare events, the respective jumps were excluded from data evaluation.

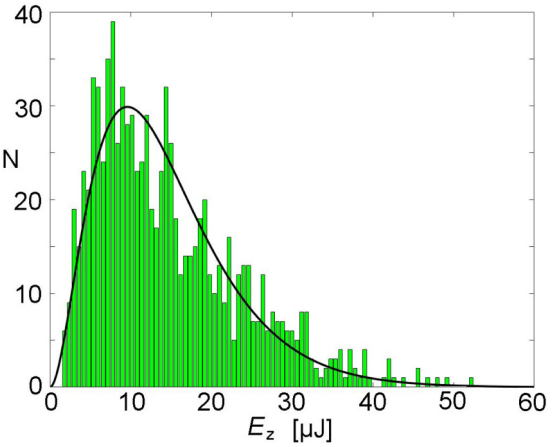

FIG. 3. Typical distribution of energies E_z of a jumping 15 mm rod excited at frequency $f = 30$ Hz, amplitude $A = 2.89$ mm ($v_{\max} = 0.545$ m/s). The average energy is 15 μJ. The high-energy tail has an exponential decay [44].

with other particles. Thus it suffices to analyze the statistics of energy and momentum transfers during individual collisions, in dependence on excitation parameters. A typical detail of a jump sequence (288 frames $\hat{=}$ 1.2 s) is depicted in Fig. 2. The parabolas describe the positions of the centers of mass; therefore they do not end at the plate positions but depend on the impact angle. It is obvious that often double impacts occur, i.e., the rod first contacts the plate with one end, then with the opposite end, before the next jump. This process is identified as the main reason for the lower excitation of rotational degrees of freedom as compared to the kinetic energy of translational motion normal to the plate, as discussed later (cf. Fig. 8). We did not evaluate the sign of the angular frequency ω here, which is irrelevant for the rotational energies. In practice, rotation changes sign between most jumps. The azimuthal angle is not conserved.

Figure 3 shows a typical distribution of the energy E_z (total potential energy and kinetic energy of the vertical motion) for a selected set of excitation parameters. The mean energy is $E_z = 15\,\mu$J. The high-energy tail is exponential as expected [44]. At low energies, a typical maximum is found near $2E_z/3$. An empirical distribution function $p(\tilde{E}_z) = \tilde{E}_z^2/(2E_0^3)\exp(-\tilde{E}_z/E_0)$ with $E_0 = 5\mu$J is shown for comparison. This function reproduces some typical features of the distributions, but it does not have a theoretical background nor does it fit in detail. Qualitatively similar observations, in particular the high-frequency characteristics, were reported by Wright *et al.* [44].

Warr *et al.* [37] analyzed rebound velocities of jumping spherical beads, and even though their behavior is expected to differ qualitatively from the jumping rods, one may compare the proposed distribution density for rebound velocities v:

$$p(v) = v^{2\beta/\langle\Phi^2\rangle}\exp\left[\frac{(\varepsilon-1)v^2}{\langle\Phi^2\rangle}\right], \tag{1}$$

with two parameters given as $\Phi = (1+\varepsilon)^2 v_{\max}^2/2$ and $\beta = (1+\varepsilon)v_{\max}^2/2$. For the distribution of energies this yields

$$p(E_z) \propto E_z^{\frac{(1-\varepsilon)}{2(1+\varepsilon)}}\exp\left[\frac{4(\varepsilon-1)E_z}{(1+\varepsilon)^2 m v_{\max}^2}\right]. \tag{2}$$

The low-energy part of this distribution, determined essentially by the exponent of the energy prefactor, is clearly different from our results for rods. The exponential high-energy tail is qualitatively similar, but the exponent is larger by a factor 4 in the rod experiments.

Figure 4 maps energies of subsequent jumps. It evidences correlations between subsequent jump heights (higher energy jumps are more likely followed by higher energy jumps), but few correlations of the rotation energies of subsequent jumps. The correlation coefficient of $E_z(n)$ and $E_z(n+1)$ of successive jumps n and $n+1$ is 0.197. The rotation energies of subsequent jumps are much weaker correlated, with a coefficient 0.06.

B. Efficiency of excitation

The total energies for different excitation parameter sets are shown in Figs. 5 and 6. First, we present separately the dependence of the total average energy on the frequency f for fixed amplitude (a) and on the amplitude A for fixed frequency (b). Two regions are excluded from experimental access: When the maximum plate acceleration $\Gamma_{\max}$ is lower than the gravitational acceleration in our experiment (vertical dotted lines), a rod lying on the plate will never lift from it. Practically, the excitation threshold is close to that value [44]. Another lower bound is given by the kinetic energy of a rod at rest on the vibrating plate. If the rod moves with the plate without jumps, it has an averaged "zero kinetic energy" estimated as $E_0 = mv_{\max}^2/4$. This E_0 roughly marks a lower boundary to measurable energies. For the long rods, that boundary is sketched in the figures by dotted parabolas. [1] Solid symbols represent the longer 15 mm rods, open symbols

[1] In microgravity, these thresholds do not exist.

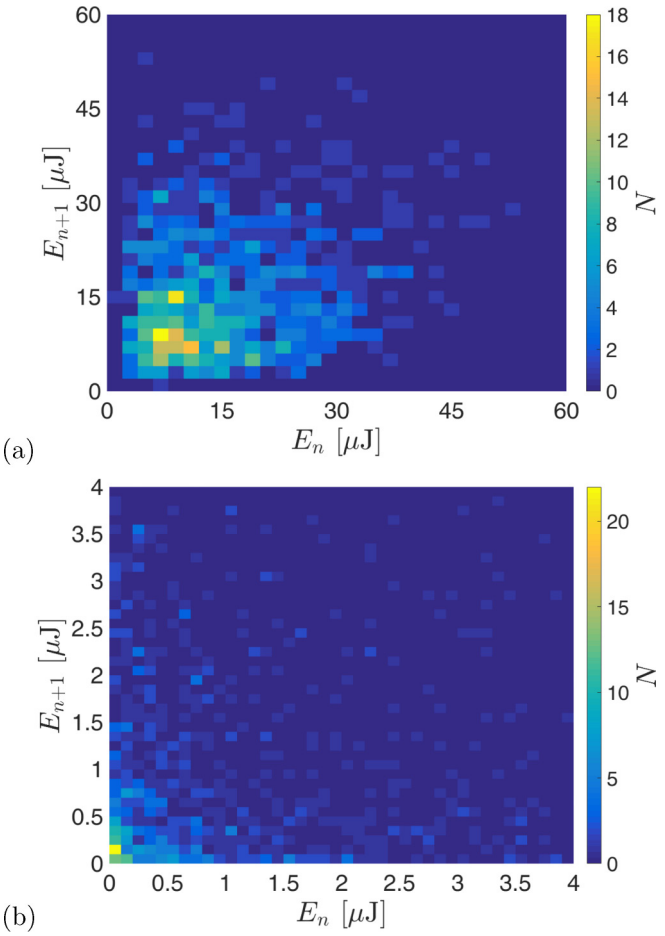

FIG. 4. Correlations of energies E_z (a) and E_{rot} (b) between successive jumps. The vertical velocities show correlations while the rotations are in good approximation uncorrelated.

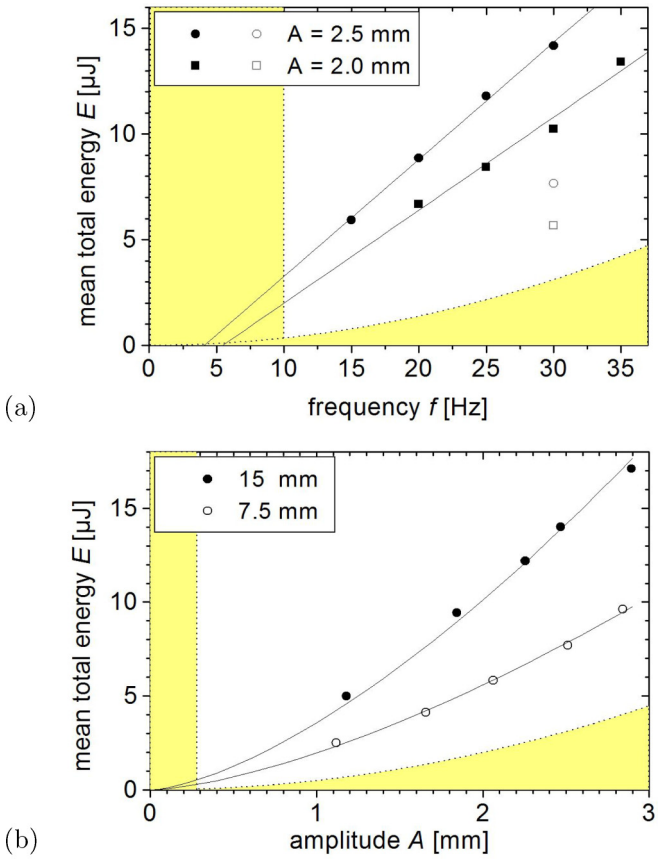

FIG. 5. Selected frequency dependencies at fixed amplitudes $A = 2$ mm and $A = 2.5$ mm (a) and amplitude dependencies at fixed frequency $f = 30$ Hz (b) for the two types of rods. The frequency characteristics can be assumed nearly linear, whereas the amplitude dependence is clearly nonlinear. The ratio of total energies E of long (solid symbols) and short (open symbols) rods is slightly smaller than their mass ratio, i.e., the efficiency of excitation is slightly better for the short pieces. Dashes mark ranges that are not accessible by experiment (see text).

the shorter 7.5 mm rods. The ratio of total mean energies at the same excitation parameters should ideally be 2, the mass ratio. In practice, it is lower by about 8%–10%. The excitation of longer rods is obviously somewhat less efficient.

In Fig. 5(a), the total mean energy is plotted as a function of f. Since measurements for different f were not at exactly the same amplitudes A, we performed a linear interpolation between the two closest amplitude data points of a given frequency. The $E(f)$ dependencies [Fig. 5(a)] for constant A can be fitted with linear functions. Even though satisfactory offset-free fits can be found (yet we see no reasonable argument for that), the best linear fits have slight offset. The slopes dE/df depend upon the amplitudes: 0.55 μJs for $A = 2.5$ mm and 0.44 μJs for $A = 2.0$ mm (solid lines). Offsets are 4.1 and 5.4 Hz, respectively. A slight nonlinearity may be present, but the experimental accuracy is not sufficient for a precise determination of the functional dependence. Best fits with functions $E(f) \propto f^{\gamma}$ yield exponents γ of 1.22 and 1.28, respectively, but these fits are not very robust. A square dependence as predicted in several publications for spherical particles (e.g., Refs. [37,38]) can definitely be excluded. In contrast, the amplitude dependencies [Fig. 5(b)] are clearly nonlinear; linear fits would not intersect the abscissa at the origin. A reasonable fit is obtained with functions $E \propto A^{3/2}$, shown as solid lines (with proportionality factors 3.6 μJ/mm$^{3/2}$ and 2.0 μJ/mm$^{3/2}$ for long and short rods, respectively).

The consequence of these fits should be a master curve for $E \propto A^{3/2} f$ as shown in Fig. 6(a). Amplitudes were chosen between 0.58 and 4.5 mm, frequencies between 15 and 40 Hz. The master graph is reasonably good for all frequencies except the lowest excitation at 15 Hz, which deviates systematically. The slope is 0.123 μJ mm$^{-3/2}$ s. The deviations of the low-frequency data (15 Hz) at high excitation strengths can be attributed to the substantial vibration amplitude of $\approx \pm 4.5$ mm. There the voice coil reaches its limits, and the excitation wave form begins to deviate from perfect sinusoidal shape. While this graph does not give clues to the underlying physical details, it provides a satisfactory prediction of the energy entry into a granular gas of rod-shaped grains as a function of excitation parameters, and it seems to exclude some earlier suggestions in literature. For example, it was reasonably argued from a dimensional analysis [5] that the kinetic energy in a granular gas of spheres excited

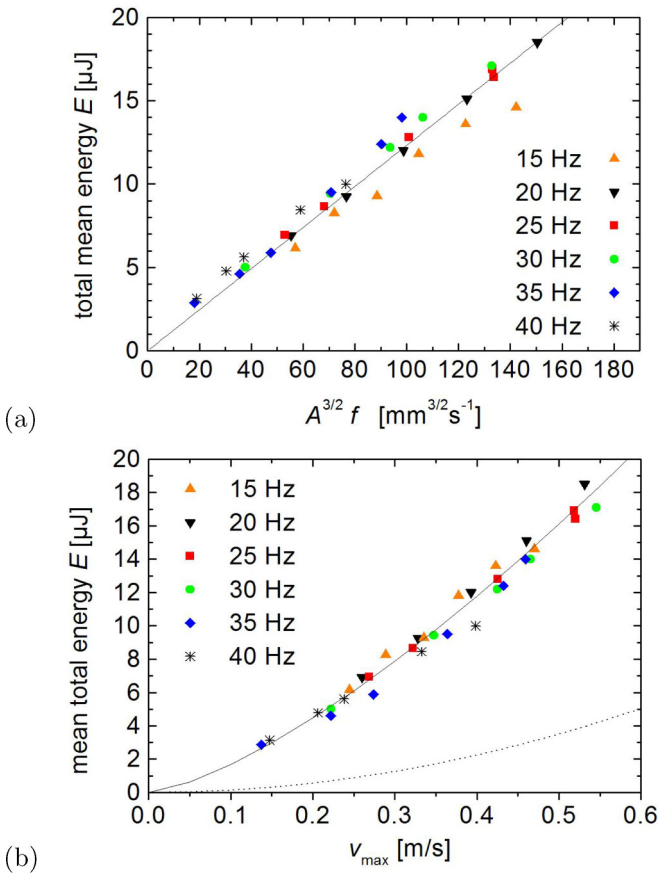

FIG. 6. Total energies of the 15 mm rods for different excitation parameters (a) as a function of $A^{3/2}f$ and (b) as a function of the maximum velocities of the moving plate, $v_{\max}$. Within experimental scattering, all data can be fitted with common master graphs (see text); only the 15 Hz curve in (a) shows some systematic deviation to less efficient driving, which is mainly a technical problem, see text. The dotted line in (b) marks the kinetic energy of a rod lying on the vibrating plate.

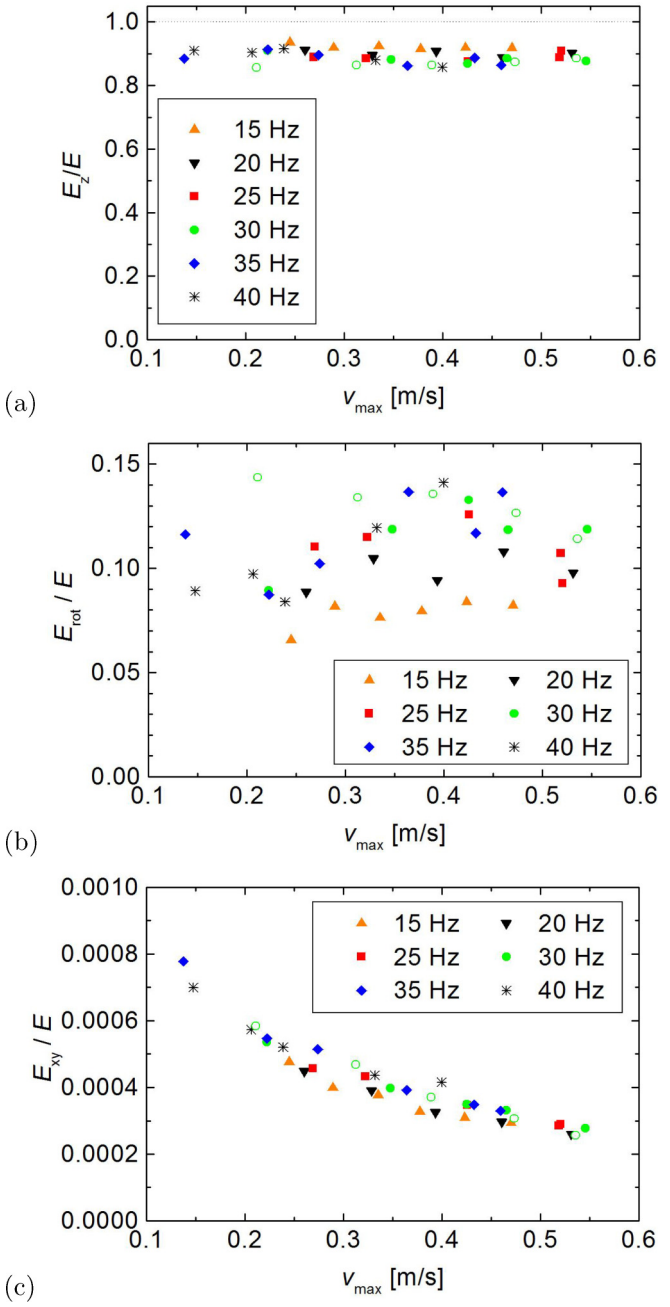

FIG. 7. Ratio of the three components and the total mean energy. The "vertical energy" E_z as the sum of kinetic energy of vertical motion and the potential energy relative to the mean plate height is shown in (a); it amounts to about 90% of the total energy. Graph (b) shows the share of rotational energy, which is of the order of 10%, irrespective of the excitation parameters. The kinetic energy of translational motions in the horizontal plane (c) is smaller by more than one order of magnitude, and a systematic decay of its share with larger excitation strengths is evident. Solid symbols: 15 mm rods; open symbols: 7.5 mm rods.

by oscillating walls should be proportional to A^2f^2. We can clearly exclude that for our rodlike particles. Other models consider maximum accelerations $\Gamma_{\max}$ [38] or the maximum velocity $v_{\max}$ as appropriate parameters. If one is interested in finding a good approximation for the dependence of the average particle energy on the plate velocity, a fairly good fit is $E = 42.5\,\mu\mathrm{J(s/m)}^{1.4}v_{\max}^{1.4}$ [Fig. 6(b)]. This is, of course, only within some experimental uncertainties compatible with the plots of Fig. 5.

C. Distribution of kinetic energy on the rotational and translational degrees of freedom

An important aspect for the investigation of driven granular gases is the distribution of kinetic energies among the degrees of freedom. In equilibrium, an equal distribution would be expected. In the mechanically driven nonequilibrium granular gas, deviations were found experimentally in the stationary state [26,29]. Partially, this can be attributed to the nonequivalent excitation of the degrees of freedom. We demonstrate this on the basis of the plots in Fig. 7.

The graphs in Fig. 7 show the ratios between the individual degrees of freedom of the jumping rod. The largest share of the mean total energy is the vertical component E_z, the sum of potential energy and motion in vertical direction (which is constant during each jump). It amounts to 90%

of the total energy. The rotational energy contributes only about 10% to the total mean energy. The graphs reveal no systematic dependence of this ratio, neither on the frequency f nor on the amplitude A. The shorter rods appear to have a slightly higher share of rotational energy, but within our experimental scattering of data of about $\pm 0.04E$, there is no clear systematic trend. Kinetic energies of horizontal motion are negligibly small. This is expected: the major momentum transfer to the jumping rods is in the vertical direction; lateral motion is not directly excited by the plate, it may originate from coupling to weak vibrational degrees of freedom of the rods.

IV. DISCUSSION AND SUMMARY

An estimation of the efficiency of the particle excitation can be made within a simple model when one assumes that the momentum change during an impact is determined by the relative velocities of plate and center of mass of the rod, the restitution coefficient, and the probability that the plate is hit in a certain phase of the oscillation. For spheres, that estimation leads to a proportionality between the square of the maximum vibrating plate velocity $v_{\max}$ and the mean energy. A similar relation has been suggested on the basis of a dimensional analysis by Falcon *et al.* [5].

Another relation suggested for jumping spheres, based on numerical and experimental data [38], was scaling of the mean energy with the form $E(\Gamma_{\max}) = \alpha\Gamma_{\max} + \beta$. These simulation results cannot easily be compared with our data since Géminard and Laroche gave only the acceleration data (in their Fig. 1), but it is not clear whether the oscillation amplitude or velocity or both were varied. An experimental graph (Fig. 3 in Ref. [38]) provides in fact an amplitude dependence. In our experiments, the two excitation parameters f and A were varied separately, and we clearly found different characteristics of $E(f)$ (nearly linear) and $E(A)$ (clearly nonlinear). Therefore, a general dependence on the plate acceleration does not exist for the rods. From our experimental data based on separate variations of plate frequency and amplitude, we have to conclude that dependence on plate velocity or acceleration can only be approximative in the rod experiments. This may reflect a general difference to jumping spheres, or demand a separate measurement of the two parameters in sphere experiments. We note that similar conclusions were drawn, in a different experiment with granular matter (a vertical shaken column of spheres), from measurements of a critical acceleration, which was found to depend on the shaking amplitude [45]. This indicates that the question regarding the role of the individual vibration parameters is more general than in the situation studied here.

An important observation is that the vibrating plate essentially excites the translational degree of motion normal to the plate, while each of the rotational degrees of freedom is more weakly excited by at least one order of magnitude. This explains why we found an excess of translational kinetic energy in earlier microgravity experiments of a permanently excited granular gas [26]. There is a simple explanation for that asymmetry: In principle, the effect of a collision of one end of the rod at rest with a vibrating plate produces an excess of rotational energy: If we assume a momentum transfer of $\Delta p = 2mv_{\text{plate}}$ [or, in the case of a restitution coefficient $\varepsilon < 1$, $\Delta p = (1+\varepsilon)mv_{\text{plate}}$] when a plate with momentary velocity v_{plate} hits one end, the kinetic energy becomes $E_z = (\Delta p)^2/(2m)$. The angular momentum transfer is $\Delta J = \Delta p\ell/2 \sin\theta$ when the rod axis is tilted by θ respective to the plate normal, the related rotational energy is $E_{\text{rot}} = (\Delta J)^2/(2I)$ with $I \approx \ell^2 m/12$. The ratio of the energies gained by a resting rod during a single impact becomes $E_{\text{rot}}/E_z = 3\sin\theta$, and on average for isotropically distributed angles θ the ratio is $E_{\text{rot}}/E_z = 2$. There are several reasons why the impact on a vibrating plate is much less effective for the excitation of rotational motions. The most important one is that many jumps are in fact double collisions: first the rod hits the plate with one end, where momentum and angular momentum are exchanged. Then, the center of mass will often continue to move towards the plate, and the rod impacts with the other end. Thereby, momentum is exchanged again, almost always additive to the first collision. The angular momentum transferred to the rod will almost exclusively oppose that of the first impact. Figure 8 visualizes such a typical event. Thus, the excitation of rotations is much less efficient than that of the vertical jump velocity.

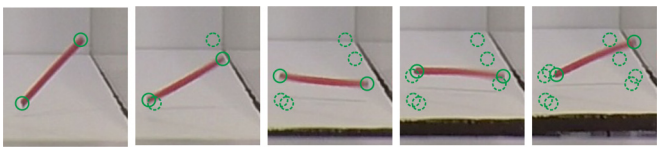

FIG. 8. Double impact, image sequence with 240 fps: the rod first touches the plate with the lower end, momentum (upward) and angular momentum (backward) are transferred. The center of mass still moves towards the plate. Then the other end touches the plate, and again momentum upward is transferred, but the angular momentum is opposite to the first impact. Green circles mark the rod ends, dashed circles mark the previous positions. The apparent slight bend of the rod in the last two images and motion blurring is a camera artifact.

An interesting aspect is the comparison with Wright's experiments [44] with bouncing rods. However, that study had a quite complementary focus, thus comparison is possible only in few details. Wright *et al.* mention only in brief that the rotational energy is much weaker than the translational energy, which is in agreement with our results. In Wright's study, the one-dimensional observation prevented a quantitative evaluation of the rotation data. The authors determined an excitation threshold for particle flips. This can be compared with our study by means of a back of the envelope estimate: The average time needed for a flip (rod performs more than a half rotation during one jump) is

$$T_{\text{flip}} \approx \pi/\omega = \pi\sqrt{\frac{I}{2E_{\text{rot}}}} \approx \pi\ell\sqrt{\frac{m}{24E_{\text{rot}}}} \tag{3}$$

with the relevant moment of inertia $I \approx m\ell^2/12$, the particle length ℓ, and mass m. The mean jump time is

$$t_{\text{j}} = 2v_0/g$$

with the mean vertical velocity $v_0 = \sqrt{2E_z/m}$. Setting the two times t_{j} and T_{flip} equal provides us with an estimate of the

threshold energy for a flip during the jump:

$$T_{\text{flip}} = \pi \ell \sqrt{\frac{m}{24 E_{\text{rot}}}} = \frac{2}{g}\sqrt{\frac{2E_z}{m}}, \tag{4}$$

$$\sqrt{E_{\text{rot}} E_z} = \frac{\pi \ell m g}{\sqrt{192}}. \tag{5}$$

If we estimate the energies (using the experimental results of Fig. 7) by $(E_{\text{rot}} E_z)^{1/2} \approx (0.1E \cdot 0.9E)^{1/2} = 0.3E$, we find

$$E_{\text{flip}} \approx 0.24 \pi \ell m g = 6.2\,\mu\text{J}$$

for the 15 mm rods, and about 1.5 μJ for the 7.5 mm rods. This simple evaluation is in qualitative agreement with Wright's results of a more than linear increase of the flip threshold with the rod length.

Another important question is the comparison of our results on single particles with the excitation of granular gases in a closed volume under microgravity conditions. That situation is more complex, because particle interactions between subsequent collisions with the plate have to be taken into account. In principle, the efficiency of excitation is similar, but one has to keep in mind that our experiment is strictly correct for isolated grains only. If the grains interact with each other in the volume, then a higher kinetic energy will lead to a higher collision rate in the container [21] and to a higher dissipation rate. This, in turn, will lead to a weaker dependence of the mean kinetic energy in the ensemble on the driving parameters. In particular, the ratio of container size and area of the vibrating wall will be relevant. The results remain valid, however, when one compares excitation parameters A and f, which yield the same E in our single-rod experiment.

Finally, we need to discuss the general validity of our observations for rods with other compositions, in particular for homogeneous rods. We have tested that with two experiments performed with homogeneous materials. The experiment performed with glass rods failed completely, because such rods charge electrostatically within a few jumps, and they finally stick to the side walls or bottom plate. Similar electrostatic charging was already mentioned in Ref. [44]. Furthermore we performed an additional experiment with copper cylinders, excited at a frequency of 30 Hz with different vibration amplitudes A between 1.2 and 2.88 mm. The results are in full qualitative agreement with those obtained with the wires. The amplitude dependence of the total energy at fixed frequency was $E \propto A^{3/2}$, clearly nonlinear, with a proportionality factor of 7.5 μJ/mm$^{3/2}$. In a loosely related system, a shaken container with a few dozen steel spheres, Warr *et al.* [46] measured the fluidization and the mean energy entry in the system. They reported rather similar velocity dependencies as for our single rod, and their scaling exponent was 1.3. The numerical simulation of a related system by Luding *et al.* [47] gave an exponent of 1.5. Even though these results are not directly comparable with the present experiment, it is interesting to see that a dependence of the excitation efficiency on the vibrating plate velocity with an exponent around 1.5 is not unusual. The share of rotational energies compared to the total kinetic energy ranged from 12% to 15%, with no systematic trend in the excitation strength dependence. This is in full accordance with the wire data. Because the bare copper surface leads to optical reflexes that disturb the image analysis and accurate particle detection, we did not perform systematic investigations of the full frequency range. It suffices to state that the amplitude dependence is the same, and the larger prefactor originates from the larger mass of the copper rods and certainly also from a different restitution coefficient.

ACKNOWLEDGMENTS

The authors acknowledge financial support by DFG within project STA 425/34-1 and by DLR within projects 50WM1241 and 50WM1344.

[1] H. M. Jaeger, S. R. Nagel, and R. P. Behringer, Granular solids, liquids, and gases, Rev. Mod. Phys. **68**, 1259 (1996).
[2] S. Luding, E. Clément, A. Blumen, J. Rajchenbach, and J. Duran, Studies of columns of beads under external vibrations, Phys. Rev. E **49**, 1634 (1994).
[3] A. Kudrolli, M. Wolpert, and J. P. Gollub, Cluster Formation Due to Collisions in Granular Material, Phys. Rev. Lett. **78**, 1383 (1997).
[4] W. Losert, D. G. W. Cooper, J. Delour, A. Kudrolli, and J. P. Gollub, Velocity statistics in excited granular media, Chaos **9**, 682 (1999).
[5] E. Falcon, R. Wunenburger, P. Évesque, S. Fauve, C. Chabot, Y. Garrabos, and D. Beysens, Cluster Formation in a Granular Medium Fluidized by Vibrations in Low Gravity, Phys. Rev. Lett. **83**, 440 (1999).
[6] E. Falcon, S. Aumaître, P. Evesque, F. Palencia, C. Lecoutre-Chabot, S. Fauve, D. Beysens, and Y. Garrabos, Collision statistics in a dilute granular gas fluidized by vibrations in low gravity, Europhys. Lett. **74**, 830 (2006).
[7] F. Rouyer and N. Menon, Velocity Fluctuations in a Homogeneous 2D Granular Gas in Steady State, Phys. Rev. Lett. **85**, 3676 (2000).
[8] A. Kudrolli and J. Henry, Non-Gaussian velocity distributions in excited granular matter in the absence of clustering, Phys. Rev. E **62**, R1489 (2000).
[9] D. L. Blair and A. Kudrolli, Velocity correlations in dense granular gases, Phys. Rev. E **64**, 050301 (2001).
[10] J. van Zon and F. C. MacKintosh, Velocity Distributions in Dissipative Granular Gases, Phys. Rev. Lett. **93**, 038001 (2004).
[11] C. C. Maaß, N. Isert, G. Maret, and C. M. Aegerter, Experimental Investigation of the Freely Cooling Granular Gas, Phys. Rev. Lett. **100**, 248001 (2008).
[12] A. T. Cadillo-Martinez and R. Sanchez, Experimental velocity distributions in a granular submonolayer, Physica A (Amsterdam) **465**, 221 (2017).
[13] P. Évesque and J. Rajchenbach, Instability in a Sand Heap, Phys. Rev. Lett. **62**, 44 (1989).
[14] K. M. Aoki, T. Akiyama, Y. Maki, and T. Watanabe, Convective roll patterns in vertically vibrated beds of granules, Phys. Rev. E **54**, 874 (1996).
[15] P. B. Umbanhowar, F. Melo, and H. L. Swinney, Localized excitations in a vertically vibrated granular layer, Nature (London) **382**, 793 (1996).

[16] M. E. Möbius, B. E. Lauderdale, S. R. Nagel, and H. M. Jaeger, Brazil-nut effect—Size separation of granular particles, Nature (London) **414**, 270 (2001).

[17] H. J. Schlichting and V. Nordmeier, Strukturen im Sand, Math. Naturwiss. Unterr. **49**, 323 (1996) (in German); J. Eggers, Sand as Maxwell's Demon, Phys. Rev. Lett. **83**, 5322 (1999).

[18] D. van der Meer, P. Reimann, K. van der Weele, and D. Lohse, Spontaneous Ratchet Effect in a Granular Gas, Phys. Rev. Lett. **92**, 184301 (2004).

[19] P. Eshuis, K. van der Weele, D. van der Meer, and D. Lohse, Granular Leidenfrost Effect: Experiment and Theory of Floating Particle Clusters, Phys. Rev. Lett. **95**, 258001 (2005).

[20] G. Wurm and J. Blum, Experiments on preplanetary dust aggregation, Icarus **132**, 125 (1998).

[21] P. K. Haff, Grain flow as a fluid-mechanical phenomenon, J. Fluid Mech. **134**, 401 (1983).

[22] E. Opsomer, M. Noirhomme, N. Vandewalle, E. Falcon, and S. Merminod, Segregation and pattern formation in dilute granular media under microgravity conditions, NPJ Microgravity **3**, 1 (2017).

[23] M. N. Bannerman, J. E. Kollmer, A. Sack, M. Heckel, P. Müller, and T. Pöschel, Movers and shakers: Granular damping in microgravity, Phys. Rev. E **84**, 011301 (2011).

[24] J. E. Kollmer, M. Tupy, M. Heckel, A. Sack, and T. Pöschel, Absence of Subharmonic Response in Vibrated Granular Systems Under Microgravity Conditions, Phys. Rev. Appl. **3**, 024007 (2015).

[25] A. Sack, M. Heckel, J. E. Kollmer, F. Zimber, and T. Pöschel, Energy Dissipation in Driven Granular Matter in the Absence of Gravity, Phys. Rev. Lett. **111**, 018001 (2013).

[26] K. Harth, U. Kornek, T. Trittel, U. Strachauer, S. Höme, K. Will, and R. Stannarius, Granular Gases of Rod-Shaped Grains in Microgravity, Phys. Rev. Lett. **110**, 144102 (2013).

[27] K. Harth, T. Trittel, U. Kornek, S. Höme, K. Will, U. Strachauer, and R. Stannarius, Microgravity experiments on a granular gas of elongated grains, AIP Conf. Proc. **1542**, 807 (2013).

[28] K. Harth, T. Trittel, K. May, S. Wegner, and R. Stannarius, Three-dimensional (3D) experimental realization and observation of a granular gas in microgravity, Adv. Space Res. **55**, 1901 (2015).

[29] K. Harth, T. Trittel, S. Wegner, and R. Stannarius, Cooling of 3D granular gases in microgravity experiments, Powders & Grains (unpublished).

[30] I. Goldhirsch and G. Zanetti, Clustering Instability in Dissipative Gases, Phys. Rev. Lett. **70**, 1619 (1993); I. Goldhirsch, M.-L. Tan, and G. Zanetti, A molecular dynamical study of granular fluids. I: The unforced granular gas in two dimensions, J. Sci. Comput. **8**, 1 (1993).

[31] T. Kanzaki, R. C. Hidalgo, D. Maza, and I. Pagonabarraga, Cooling dynamics of a granular gas of elongated particles, J. Stat. Mech. (2010) P06020; R. C. Hidalgo, I. Zuriguel, D. Maza, and I. Pagonabarraga, Granular packings of elongated faceted particles deposited under gravity, *ibid.* (2010) P06025.

[32] M. Huthmann, T. Aspelmeier, and A. Zippelius, Granular cooling of hard needles, Phys. Rev. E **60**, 654 (1999).

[33] T. Aspelmeier, G. Giese, and A. Zippelius, Cooling dynamics of a dilute gas of inelastic rods: A many particle simulation, Phys. Rev. E **57**, 857 (1998); G. Costantini, U. Marini-Bettolo-Marconi, G. Kalibaeva, and G. Ciccotti, The inelastic hard dimer gas: a nonspherical model for granular matter, J. Chem. Phys. **122**, 164505 (2005).

[34] F. Villemot and J. Talbot, Homogeneous cooling of hard ellipsoids, Granular Matter **14**, 91 (2012); S. M. Rubio-Largo, F. Alonso-Marroquin, T. Weinhart, and R. C. Hidalgo, Homogeneous cooling state of frictionless rod particles, Physica A (Amsterdam) **443**, 477 (2016).

[35] H. Pourtavakoli, E. J. R. Parteli, and T. Pöschel, Granular dampers: Does particle shape matter? New J. Phys. **18**, 073049 (2016).

[36] See, e.g., J.-Y. Chastaing, E. Bertin, and J.-C. Géminard, Dynamics of a bouncing ball, Am. J. Phys. **83**, 518 (2015); R. M. Everson, Chaotic dynamics of a bouncing ball, Physica D (Amsterdam) **19**, 355 (1986); Z. J. Kowalik, M. Franaszek, and P. Pieranski, Self-reanimating chaos in the bouncing-ball system, Phys. Rev. A **37**, 4016 (1988); J. M. Luck and A. Mehta, Bouncing ball with a finite restitution—Chattering, locking and chaos, Phys. Rev. E **48**, 3988 (1993); E. Falcon, C. Laroche, S. Fauve, and C. Coste, Behavior of one inelastic ball bouncing repeatedly off the ground, Eur. Phys. J. B **3**, 45 (1998); N. B. Tufillaro, T. Abbot, and J. Reilly, *An Experimental Approach to Nonlinear Dynamics and Chaos*, (Addison-Wesley, New York, 1992).

[37] S. Warr, W. Cooke, R. C. Ball, and J. M. Huntley, Probability distribution functions for a single-particle vibrating in one dimension: Experimental study and theoretical analysis, Physica A (Amsterdam) **231**, 551 (1996).

[38] J.-C. Géminard and C. Laroche, Energy of a single bead bouncing on a vibrating plate: Experiments and numerical simulations, Phys. Rev. E **68**, 031305 (2003).

[39] J. Atwell and J. S. Olafsen, Anisotropic dynamics in a shaken granular dimer gas experiment, Phys. Rev. E **71**, 062301 (2005).

[40] S. Dorbolo, D. Volfson, L. Tsimring, and A. Kudrolli, Dynamics of a Bouncing Dimer, Phys. Rev. Lett. **95**, 044101 (2005).

[41] S. Dorbolo, F. Ludewig, and N. Vandewalle, Bouncing trimer: A random self-propelled particle, chaos and periodical motions, New J. Phys. **11**, 033016 (2009).

[42] J. Wang, C.-S. Liu, Y.-B. Jia, and D.-L. Ma, Ratchet rotation of a 3D dimer on a vibrating plate, Eur. Phys. J. E **37**, 1 (2014).

[43] M. Hubert, F. Ludewig, S. Dorbolo, and N. Vandewalle, Bouncing dynamics of a spring, Physica D (Amsterdam) **272**, 1 (2014).

[44] H. S. Wright, M. R. Swift, and P. J. King, Stochastic dynamics of a rod bouncing upon a vibrating surface, Phys. Rev. E **74**, 061309 (2006).

[45] S. Renard, T. Schwager, T. Pöschel, and C. Salueña, Vertically shaken column of spheres: Onset of fluidization, Eur. Phys. J. E **4**, 233 (2001).

[46] S. Warr, J. M. Huntley, and G. T. H. Jacques, Fluidization of a two-dimensional granular system: Experimental study and scaling behavior, Phys. Rev. E **52**, 5583 (1995).

[47] S. Luding, H. J. Herrmann, and A. Blumen, Simulations of two-dimensional arrays of beads under external vibrations: Scaling behavior, Phys. Rev. E **50**, 3100 (1994).